Control of Decoherence: Dynamical Decoupling versus Quantum Zeno Effect
A case study for trapped ions

S. TASAKI,[1] A. TOKUSE,[1] P. FACCHI,[2] S. PASCAZIO[2]

[1]*Department of Applied Physics and Advanced Institute for Complex Systems, Waseda University, 3-4-1 Okubo, Shinjuku-ku, Tokyo 169-8555, Japan*

[2]*Dipartimento di Fisica, Università di Bari, and Istituto Nazionale di Fisica Nucleare, Sezione di Bari, I-70126 Bari, Italy*

Received 26 March 2003; accepted 27 October 2003
Published online 14 January 2004 in Wiley InterScience (www.interscience.wiley.com).
DOI 10.1002/qua.10870

ABSTRACT: The control of thermal decoherence via dynamical decoupling and via the quantum Zeno effect (Zeno control) is investigated for a model of trapped ion, where the dynamics of two low-lying hyperfine states undergoes decoherence due to the thermal interaction with an excited state. Dynamical decoupling is a procedure that consists in periodically driving the excited state, while the Zeno control consists in frequently measuring it. When the control frequency is high enough, decoherence is shown to be suppressed. Otherwise, both controls may accelerate decoherence. © 2004 Wiley Periodicals, Inc. Int J Quantum Chem 98: 160–172, 2004

Key words: quantum computing; decoherence control; quantum Zeno effect; dynamical decoupling; ion trap

1. Introduction

The theory of quantum information and computation has provided various promising ideas, such as substantially faster algorithms than their classical counterparts and very secure cryptography [1]. Examples are Shor's factorizing algorithm [2] and Grover's search algorithm [3], where several computational states are simultaneously described by a single wave function and parallel information processing is carried out by unitary operations. Moreover, some of the basic steps have already been experimentally realized: basic operations for quantum computation were realized with trapped ions [4, 5] and with the nuclear spins of organic molecules [6]. Shor's algorithm for factorizing $Z = 15$ was investigated with the nuclear spins of organic molecules [7].

Correspondence to: S. Tasaki; e-mail: stasaki@waseda.jp
Contract grant sponsors: Japan Society for the Promotion of Science (JSPS); Ministry of Education, Culture, Sports, Science, and Technology of Japan.

The essential ingredient for the efficiency of quantum algorithms and cryptography is the principle of superposition of states. As pointed out, e.g., by Unruh [8], the loss of purity (i.e., decoherence) of states would deteriorate the performance, particularly in the case of large scale computations or of long-distance communications. Thus, the information carried by a quantum system has to be protected from decoherence. So far, several schemes have been proposed, such as the use of quantum error-correcting codes [9], the use of decoherence-free subspaces and/or noiseless subsystems [10], and the quantum dynamical decoupling [11–15].

Quantum dynamical decoupling was proposed by Viola and Lloyd [11], with the system periodically driven with period T_c in an appropriate manner so that the target subsystem is decoupled from the environment. It was shown [11, 12] that complete decoupling is achieved in the $T_c \to 0$ limit, or the limit of infinitely fast control. The procedure is simpler than the other methods because one only has to drive the system periodically. However, as it is not possible to achieve the $T_c \to 0$ limit, its performance for nonvanishing T_c should be investigated. Such studies were carried out for a two-level system in an environment via a system–energy-preserving interaction [11] and for a harmonic oscillator coupled with an environment [14]. In the present study, we provide one more example, namely a model of a trapped ion used in [4]. This model explicitly involves a unitary operation for the quantum-state manipulation, which was not included in the previous models.

The key ingredient of dynamical decoupling is the continuous disturbance of the system, which suppresses the system–environment interaction. As already pointed out by Viola and Lloyd [11], the situation is similar to the so-called quantum Zeno effect, where frequent measurements of a system suppress quantum transitions [16–18] (for recent reviews, see [19]). This phenomenon is more general than originally thought: a nontrivial time evolution may occur in the case of frequent measurements in an appropriate setting. Namely, when the measurement process is described by a multidimensional projection operator, frequent measurements restrict the evolution within each subspace specified by the projection operator and a superselection rule dynamically arises [20]. Therefore, if one can design the measurement process so that different superselection sectors (defined by the given measurements) are coupled by the interaction between a target system and the environment, the system-environment interaction can be suppressed by frequent measurements. We refer to such a decoherence control as a quantum Zeno control. Since, in the case of the quantum Zeno experiment by Itano and others [17, 18], the measurement process was realized as a dynamical process, namely the optical pulse irradiation, it is interesting to compare the two procedures (the quantum Zeno control and the quantum dynamical decoupling) for a model of trapped ion. This is one of the objectives of this article.

This article is organized as follows. In section 2, the quantum dynamic decoupling and the quantum Zeno control are briefly reviewed. In section 3, we introduce a model of the trapped ion, which takes into account the unitary Rabi oscillation and thermal decoherence. The dynamical decoupling and Zeno controls of this model are discussed, respectively, in sections 4 and 5. After a discussion of the cases of infinitely fast controls, the effects of the finiteness of the control period are investigated. It is shown that both controls may accelerate decoherence if they are not sufficiently fast. This implies the necessity of a careful design of the control and a careful study of the timescales involved. The last section is devoted to conclusions.

2. Quantum Dynamical Decoupling and Quantum Zeno Control

2.1. SYSTEM

The total system consists of a target system and a reservoir and its Hilbert space $\mathcal{H}_{\text{tot}}$ is the tensor product of the system Hilbert space, $\mathcal{H}_S$, and the reservoir Hilbert space, $\mathcal{H}_B$: $\mathcal{H}_{\text{tot}} = \mathcal{H}_S \otimes \mathcal{H}_B$. The total Hamiltonian H_{tot} is the sum of the system part $H_S \otimes \mathbf{1}_B$, the reservoir part $\mathbf{1}_S \otimes H_B$ and their interaction H_{SB}, which is responsible for decoherence:

$$H_{\text{tot}} = H_S \otimes \mathbf{1}_B + \mathbf{1}_S \otimes H_B + H_{SB}(t) \qquad (1)$$

Operators $\mathbf{1}_S$ and $\mathbf{1}_B$ are the identity operators, respectively, in the Hilbert spaces $\mathcal{H}_S$ and $\mathcal{H}_B$, and the operators H_S and H_B act, respectively, on $\mathcal{H}_S$ and $\mathcal{H}_B$. Here, in order to discuss controls in an interaction picture, a time-dependent interaction is considered.

Since, in general, the reservoir state is mixed, it is convenient to describe the time evolution in terms of density matrices. In the case of a quantum state manipulation, the initial state $\rho(0)$ is set to be a tensor

product of a system initial state $\sigma(0)$ and a reservoir (usually equilibrium) state ρ_B: $\rho(0) = \sigma(0) \otimes \rho_B$. The system state $\sigma(t)$ at time t is given by the partial trace of the state $\rho(t)$ of the whole system with respect to the reservoir degrees of freedom: $\sigma(t) \equiv \mathrm{tr}_B \rho(t)$. When $\sigma(t)$ is not unitarily equivalent to $\sigma(0)$ for a given class of initial states, decoherence is said to appear. The purpose of the control is to suppress such decoherence. For the decoherence control, it is sufficient to consider only those initial states that are relevant to the quantum state manipulation in question, but not to all states.

2.2. QUANTUM DYNAMICAL DECOUPLING

Here we slightly generalize the arguments of [12] (see also [14]). This control is carried out via a time-dependent system Hamiltonian $H_c(t)$:

$$H(t) = H_{\mathrm{tot}} + H_c(t) \otimes \mathbf{1}_B, \tag{2}$$

where $H_c(t)$ is designed so that a time-ordered exponential $U_c(t) \equiv \mathcal{T} \exp\{-i \int_0^t H_c(s)ds\}$ satisfies

(A) $U_c(t)$ is periodic with period T_c; $U_c(t + T_c) = U_c(t)$.
(B) $\int_0^{T_c} dt (U_c^\dagger(t) \otimes \mathbf{1}_B) H_{SB}(t + s)(U_c(t) \otimes \mathbf{1}_B) = O(T_c^{1+\epsilon})$, $(0 < \epsilon \leq 1$, T_c: small, $\forall s)$.

Going to the interaction picture where $H_c(t)$ is unperturbed, the density matrix at time $T = NT_c$ with an initial state $\rho(0)$ is given by $\rho(T) = U_{\mathrm{tot}}(NT_c)\rho(0)U_{\mathrm{tot}}^\dagger(NT_c)$, where

$$U_{\mathrm{tot}}(NT_c) = \mathcal{T} \exp\left[-i \int_0^{NT_c} \tilde{H}_{\mathrm{tot}}(s)ds\right] = \prod_{m=1}^{N} \left\{\mathcal{T} \exp\left[-i \int_{(m-1)/T_c}^{mT_c} \tilde{H}_{\mathrm{tot}}(s)ds\right]\right\} \tag{3}$$

and $\tilde{H}_{\mathrm{tot}}(t) = (U_c^\dagger(t) \otimes \mathbf{1}_B) H_{\mathrm{tot}}(U_c(t) \otimes \mathbf{1}_B)$. A standard Magnus expansion of the time-ordered exponential [23] leads to

$$\mathcal{T} \exp\left\{-i \int_{(m-1)T_c}^{mT_c} \tilde{H}_{\mathrm{tot}}(s)ds\right\} = e^{-i[\bar{H}_m^{(0)} + \bar{H}_m^{(1)} + \cdots]T_c}, \tag{4}$$

where $\bar{H}_m^{(0)} \equiv (1/T_c) \int_{(m-1)T_c}^{mT_c} \tilde{H}_{\mathrm{tot}}(s)ds$ and the rest terms $\bar{H}_m^{(j)}$ are of the order of T_c^j $(j = 1, 2, \cdots)$.

By assumption (B), one has $\bar{H}_m^{(0)} = \bar{H}^{(0)} + O(T_c^\epsilon)$, where

$$\bar{H}^{(0)} = \bar{H}_S \otimes \mathbf{1}_B + \mathbf{1}_S \otimes H_B, \tag{5}$$

$\bar{H}_S \equiv (1/T_c) \int_0^{T_c} dt U_c^\dagger(t) H_S U_c(t)$, and they are independent of T_c because $U_c(t)$ is T_c-periodic. Therefore, in the limit $T_c \to 0$, while keeping $T = NT_c$ constant, one obtains

$$U_{\mathrm{tot}}(T) \simeq \left[1 - i\bar{H}^{(0)} \frac{T}{N} + O\left(\frac{1}{N^{1+\epsilon}}\right)\right]^N \xrightarrow{N \to \infty} e^{-i\bar{H}_S T} \otimes e^{-iH_B T}. \tag{6}$$

In short, as a result of the infinitely fast control, the system–reservoir coupling is eliminated and, thus, decoherence is suppressed. Note that if one designs H_c so that

$$U_c(t) \equiv g_j \quad \left(\frac{j-1}{M} T_c \leq t < \frac{j}{M} T_c \,;\, j = 1, \cdots, M\right), \tag{7}$$

where $\{g_j\}$ is a set of unitary operators acting on $\mathcal{H}_S$, $\bar{H}_S$ becomes

$$\bar{H}_S = \frac{1}{M} \sum_{j=1}^{M} g_j^\dagger H_S g_j. \tag{8}$$

The relation between the dynamical decoupling with the prescription (7) and a symmetry group was discussed in [13].

2.3. QUANTUM ZENO CONTROL

Now we turn to the Zeno control by adapting the argument of [20]. This control is performed by frequent measurements of the system. The most general measurement is described by a projection operator acting on the density matrix:

$$\rho \to \hat{P}\rho \equiv \sum_n (P_n \otimes \mathbf{1}_B)\rho(P_n \otimes \mathbf{1}_B). \tag{9}$$

where $\{P_n\}$ is a set of orthogonal Hermitian projection operators acting on $\mathcal{H}_S$. In the following, we restrict ourselves to the case where the measuring apparatus does not "select" different outcomes (nonselective measurement) [21] and the projection

operators are complete; $\Sigma_n P_n = \mathbf{1}_S$. As in the dynamical decoupling, the measurement is designed so that

$$(C) \quad \hat{P}H_{SB}(t) = \sum_n (P_n \otimes \mathbf{1}_B) H_{SB}(t)(P_n \otimes \mathbf{1}_B) = 0.$$

The Zeno control consists in performing repeated nonselective measurements at times $t = nT_c$ ($n = 0, 1, 2, \cdots$). Between successive measurements, the system evolves via H_{tot}. In terms of the Liouville operator $\mathcal{L}_{\text{tot}}$ defined by $\mathcal{L}_{\text{tot}}\rho \equiv [H_{\text{tot}}, \rho] = H_{\text{tot}}\rho - \rho H_{\text{tot}}$, the density matrix $\rho(NT_c)$ after $N + 1$ measurements with an initial state $\rho(0)$ is given by

$$\rho(NT_c) = \prod_{m=1}^{N} \{\hat{P}\mathcal{T} e^{-i\int_{(m-1)T_c}^{mT_c} \mathcal{L}_{\text{tot}}(t)dt}\hat{P}\}\rho(0). \quad (10)$$

Assumption (C) yields

$$\hat{P}\int_{(m-1)T_c}^{mT_c} \mathcal{L}_{\text{tot}}(t)dt\hat{P}\rho = \hat{P}\int_{(m-1)T_c}^{mT_c} [\hat{P}H_{\text{tot}}(t), \rho]dt$$
$$= T_c\hat{P}[\bar{H}'_S \otimes \mathbf{1}_B + \mathbf{1}_S \otimes H_B, \rho] \equiv T_c\bar{\mathcal{L}}^{(0)}\rho,$$

and, thus, in the limit $T_c \to 0$ while keeping $T = NT_c$ constant, we get

$$\rho(NT_c) \simeq \hat{P}\prod_{m=1}^{N}\left\{\left[\mathbf{1} - i\hat{P}\int_{(m-1)T_c}^{mT_c} \mathcal{L}_{\text{tot}}(t)\hat{P}dt\right]\right\}\rho(0)$$
$$\simeq \hat{P}\left\{\left[1 - i\bar{\mathcal{L}}^{(0)}\frac{T}{N}\right]\right\}^N \rho(0) \to \hat{P}e^{-i\bar{\mathcal{L}}^{(0)}T}\rho(0)$$
$$= \hat{P}(e^{-i\bar{H}'_S T} \otimes e^{-iH_B T}\rho(0)e^{-i\bar{H}'_S T} \otimes e^{iH_B T}), \quad (11)$$

where the controlled system Hamiltonian $\bar{H}'_S$ is given by

$$\bar{H}'_S \equiv \sum_n P_n H_S P_n. \quad (12)$$

Hence, as a result of infinitely frequent measurements, the system–reservoir coupling is eliminated and, thus, decoherence is suppressed. Note the similarity between the controlled system Hamiltonians for a particular dynamical decoupling (8) and for the Zeno control (12). This is not a mere coincidence. Indeed, one can show that, by enlarging the Hilbert space so that the original measurement process is expressed by a dynamical process in the larger space, the two controls are equivalent. This will be discussed in detail elsewhere. However, throughout this article, dynamical decoupling refers to a situation in which the evolution is coherent (unitary) and the Zeno control to a situation in which the evolution involves incoherent processes such as measurements.

3. Two-Level System With Thermal Decoherence

3.1. MODEL

We consider the model of a trapped Be ion used in [4] (see also [17]). Here we assume that the ion is at rest and consider only the dynamics of the hyperfine states. The main mechanism of decoherence can then be attributed to the emission and absorption of thermal photons associated with transitions to nearby excited states. For the sake of simplicity, one of the hyperfine states is assumed to couple electromagnetically with a nearby excited state (Fig. 1), the polarization of the photon is neglected and only the rotating terms (i.e., the slowly varying terms in the interaction picture) are taken into account (rotating wave approximation) for the driven parts.

Let $|1\rangle$, $|2\rangle$, and $|3\rangle$ be the lower hyperfine, upper hyperfine, and excited states, respectively, and $a_{\mathbf{k}}$ the annihilation operator of a photon with wavevector $\mathbf{k}$ and energy $\omega_k = c|\mathbf{k}|$ (c: speed of light). Then, the Hamiltonian is given by

$$H_{\text{tot}}(t) = H_S(t) \otimes \mathbf{1}_B + \mathbf{1}_S \otimes H_B + \lambda H_{SB} \quad (13)$$

$$H_S(t) = \omega_2|2\rangle\langle 2| + \omega_3|3\rangle\langle 3| + \lambda^2\{\Delta e^{i\omega'_2 t}|1\rangle\langle 2| + (h.c.)\}, \quad (14)$$

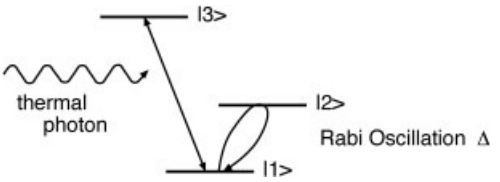

FIGURE 1. Schematic diagram of the system. $|1\rangle$, $|2\rangle$, and $|3\rangle$ are the lower hyperfine, upper hyperfine, and excited states, respectively.

$$H_B = \int d^3\mathbf{k}\,\omega_k a_\mathbf{k}^\dagger a_\mathbf{k} \tag{15}$$

$$H_{SB} = \int d^3\mathbf{k} V_k(|1\rangle\langle 3| + |3\rangle\langle 1|) \otimes (a_\mathbf{k}^\dagger + a_\mathbf{k}). \tag{16}$$

The bare energies ω_2 and ω_3 of states $|2\rangle$ and $|3\rangle$ are measured from that of the lower hyperfine state $|1\rangle$ ($\omega_1 = 0$). The third term of (14) represents the rf control of the Rabi oscillation and the amplitude $\lambda^2\Delta$ corresponds to the Rabi frequency. Because of the Lamb shift, the energy difference between the two hyperfine states ω_2' is different from ω_2 and the frequency of the irradiated field should be so tuned that it resonates with ω_2'. The function V_k is assumed to behave like

$$V_k = \sqrt{\frac{v_0^2 c^3}{8\pi^2\omega_k}}\, e^{-(\omega_k/2\omega_c)}, \tag{17}$$

with a cutoff frequency ω_c and a dimensionless strength v_0. The dimensionless coupling constant λ measures the relative order of magnitude of each term and is of order $\sqrt{\gamma_e/\omega_3}$, where γ_e is the inverse lifetime of the excited state. For the system in [4], typical order of magnitudes of the frequencies are $\gamma_e/\omega_3 \simeq 10^{-8}$ and (Rabi frequency)$/\omega_3 \simeq 10^{-10}$, which imply that $\lambda \simeq 10^{-4}$ and the Rabi frequency are of order λ^2. It is also reported that the decoherence time is longer than the Rabi period by two orders of magnitude [4].

It is convenient to move to a rotating frame with the aid of the unitary operator

$$U_R(t) = \exp\{i(\lambda^2\delta|1\rangle\langle 1| + \omega_2|2\rangle\langle 2| + \omega_3|3\rangle\langle 3|)t\} \otimes \exp\left\{i\omega_3' t \int d^3\mathbf{k} a_\mathbf{k}^\dagger a_\mathbf{k}\right\}$$

where $\lambda^2\delta = \omega_2 - \omega_2'$ and $\omega_3' = \omega_3 - \lambda^2\delta$. Then the transformed Hamiltonian H_{tot}^R is

$$H_{\text{tot}}^R \equiv i\frac{\partial U_R(t)}{\partial t} U_R^\dagger(t) + U_R(t) H_{\text{tot}}(t) U_R^\dagger(t) = \lambda^2 H_S^R \otimes \mathbf{1}_B + \mathbf{1}_S \otimes H_B^R + \lambda H_{SB}^R(t), \tag{18}$$

$$H_S^R = -\delta|1\rangle\langle 1| + \{\Delta|1\rangle\langle 2| + (h.c.)\}, \tag{19}$$

$$H_B^R = \int d^3\mathbf{k}(\omega_k - \omega_3')a_\mathbf{k}^\dagger a_\mathbf{k}, \tag{20}$$

$$H_{SB}^R(t) = \int d^3\mathbf{k} V_k|1\rangle\langle 3| \otimes (a_\mathbf{k}^\dagger + e^{-2i\omega_3' t} a_\mathbf{k}) + (h.c.). \tag{21}$$

This is our starting point.

3.2. DECOHERENCE

We consider the time evolution starting from an initial state given by the tensor product of a system initial state and the reservoir equilibrium state with inverse temperature β:

$$i\frac{\partial\rho(t)}{\partial t} = \{\mathcal{L}_B + \lambda\mathcal{L}_{SB}(t) + \lambda^2\mathcal{L}_S\}\rho(t) \tag{22}$$

$$\rho(0) = \sigma(0) \otimes \rho_B \tag{23}$$

$$\rho_B = \frac{1}{Z}\exp(-\beta H_B) \tag{24}$$

where Z is the normalization constant and the operators $\mathcal{L}_B$, $\mathcal{L}_{SB}$, and $\mathcal{L}_S$ are defined by

$$\mathcal{L}_B\rho \equiv [\mathbf{1}_S \otimes H_B^R, \rho]$$
$$\mathcal{L}_{SB}(t)\rho \equiv [H_{SB}^R(t), \rho] \quad \mathcal{L}_S\rho \equiv [H_S^R \otimes \mathbf{1}_B, \rho] \tag{25}$$

Since the time scale of the quantum state manipulation is of the same order of magnitude as the Rabi period ($\sim\lambda^{-2}$) and is very long compared with $1/\omega_3(\sim\lambda^0)$, the process is well described by the van Hove limit approximation [24, 25]. The starting point is the decomposition of the Liouville equation (22), with the aid of a projection operator

$$\mathcal{P}\rho \equiv (\text{tr}_B\rho) \otimes \rho_B \tag{26}$$

where tr_B stands for the partial trace over the reservoir degrees of freedom and ρ_B is the equilibrium reservoir state (24). Then, in the limit $\lambda \to 0$, while keeping $\tau = \lambda^2 t$ constant, the reduced density matrix $\sigma \equiv \text{tr}_B\rho$ is found to satisfy [24–26]

$$\frac{\partial\sigma}{\partial\tau} = -i\Lambda\sigma \tag{27}$$

where we have used $\mathcal{P}\mathcal{L}_B\mathcal{P} = 0$ and

$$-i\Lambda\sigma = -i[H_S^R, \sigma] - \int_0^{+\infty} dt \lim_{\lambda\to 0} \mathrm{tr}_B \left\{ \mathscr{L}_{SB}\left(\frac{\tau}{\lambda^2}\right) e^{-i\mathscr{L}_B t} \mathscr{L}_{SB} \times \left(\frac{\tau}{\lambda^2} - t\right) e^{i\mathscr{L}_B t} \sigma(\tau) \otimes \rho_B \right\}$$

$$= -i[\delta' |3\rangle\langle 3| + \Delta[|1\rangle\langle 2| + (h.c.)], \sigma] + \gamma_e |1\rangle\langle 3|\sigma|3\rangle\langle 1| + \gamma_d |3\rangle\langle 1|\sigma|1\rangle\langle 3| - \left\{ \frac{\gamma_d}{2} |1\rangle\langle 1| + \frac{\gamma_e}{2} |3\rangle\langle 3|, \sigma \right\} \quad (28)$$

with $\{,\}$ the anti-commutator. In the above, the limit $\lambda \to 0$ should be understood to drop terms that oscillate with frequencies $\sim\lambda^{-2}$ (cf. [25]). The parameter δ is chosen as

$$\delta = p.v. \int_{-\infty}^{+\infty} d\omega \, \frac{\kappa_d(\omega)}{\omega - \omega_3'} \quad (29)$$

and δ', γ_d, and γ_e are given by

$$\delta' = -p.v. \int_{-\infty}^{+\infty} d\omega \, \frac{\kappa_e(\omega)}{\omega - \omega_3'} \quad (30)$$

$$\gamma_d = 2\pi\kappa_d(\omega_3'), \qquad \gamma_e = 2\pi\kappa_e(\omega_3') \quad (31)$$

where

$$\kappa_d(\omega) = \kappa_e(\omega) e^{-\beta\omega} = \int d^3\mathbf{k} \, \frac{V_k^2 \delta(\omega_k - \omega)}{e^{\beta\omega_k} - 1} = \frac{v_0^2}{2\pi} \frac{\omega e^{-|\omega|/\omega_c}}{e^{\beta\omega} - 1} \quad (32)$$

are the thermal spectral density functions (form factors). The symbol *p.v.* in front of the integrals indicates Cauchy's principal value.

In terms of the matrix elements $\sigma_{ij} \equiv \langle i|\sigma|j\rangle$, one has $\sigma_{21} = \bar{\sigma}_{12}$ and

$$\frac{\partial\sigma_{11}}{\partial\tau} = -i\Delta\{\sigma_{21} - \sigma_{12}\} - \gamma_d\sigma_{11} + \gamma_e\sigma_{33} \quad (33)$$

$$\frac{\partial\sigma_{12}}{\partial\tau} = -i\Delta\{\sigma_{22} - \sigma_{11}\} - \frac{\gamma_d}{2}\sigma_{12} \quad (34)$$

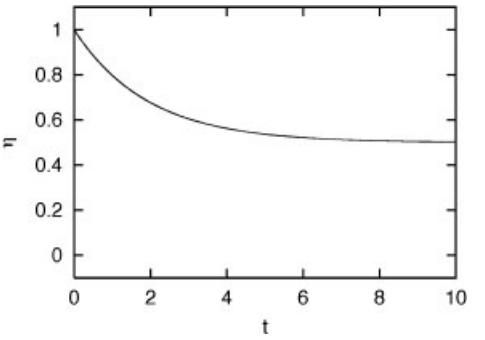

FIGURE 2. Time evolution of the purity η of the target states. The time unit on the horizontal axis is the decoherence time γ_d^{-1}.

$$\frac{\partial\sigma_{22}}{\partial\tau} = i\Delta\{\sigma_{21} - \sigma_{12}\} \quad (35)$$

$$\frac{\partial\sigma_{33}}{\partial\tau} = \gamma_d\sigma_{11} - \gamma_e\sigma_{33}. \quad (36)$$

The purity of the target states is measured by $\eta \equiv \sigma_{11}^2 + \sigma_{22}^2 + 2|\sigma_{12}|^2$, as $\eta = 1$ for pure superpositions of $|1\rangle$ and $|2\rangle$, and $\eta < 1$ for states involving the irrelevant state $|3\rangle$ or mixed states. Figure 2 shows the evolution of the quantity $\eta(t)$ starting from $\sigma(0) = |1\rangle\langle 1|$ for $\Delta = 100\gamma_d$, $\gamma_e = 1000\gamma_d$. As time goes on, the purity η of the target states is lost, or decoherence takes place. One clearly sees that the decoherence time scales as $1/\gamma_d$.

4. Control of Thermal Decoherence Via Dynamical Decoupling

We consider a dynamical decoupling control of the thermal decoherence discussed in the previous section. Since decoherence arises from the transition between the states $|1\rangle$ and $|3\rangle$ associated with absorption and emission of photons, it is expected to be suppressed if $|3\rangle$ does not contribute to the $|1\rangle$–$|2\rangle$ dynamics. So we consider a control via the Rabi oscillation between the state $|3\rangle$ and a higher excited state $|4\rangle$ (cf. Fig. 3), which is described by

$$H_c(t) = \Omega e^{i(\omega_4 + \xi)t} |3\rangle\langle 4| + (h.c.), \quad (37)$$

where ω_4 is the energy of the state $|4\rangle$, and Ω and ξ are real parameters. Since there exists one more state, a term $\omega_4|4\rangle\langle 4| \otimes \mathbf{1}_B$ should be added to the

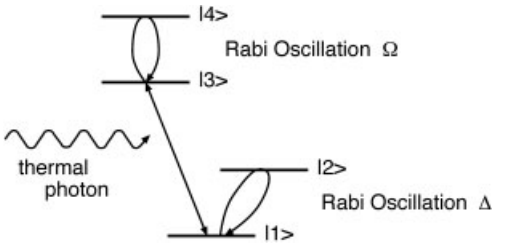

FIGURE 3. Schematic representation of the system under the quantum dynamical decoupling control.

Hamiltonian H_S. As a result, the following Liouvillian should be added

$$\{\Delta\mathcal{L}_S + \mathcal{L}_c(t)\}\rho \equiv [(\omega_4|4\rangle\langle 4| + H_c(t)) \otimes \mathbf{1}_B, \rho], \tag{38}$$

and the evolution equation reads

$$\frac{\partial\rho}{\partial t} = \{\mathcal{L}_B + \Delta\mathcal{L}_S + \mathcal{L}_c(t) + \lambda\mathcal{L}_{SB}(t) + \lambda^2\mathcal{L}_S\}\rho(t). \tag{39}$$

4.1. IDEAL DYNAMIC DECOUPLING

The evolution operator $U_c(t)$ generated by the control Hamiltonian $H_c(t)$ is given by

$$U_c(t) = \mathcal{T}\exp\left[-i\int_0^t dt' H_c(t')\right]$$
$$= e^{-i(\omega_4+\xi)|4\rangle\langle 4|t}\exp[-i\{-(\omega_4+\xi)|4\rangle\langle 4| + \Omega[|3\rangle\langle 4| + (h.c.)]\}t]. \tag{40}$$

When restricting to a subspace spanned by $|3\rangle$ and $|4\rangle$, the second factor is a sum of two oscillating projection operators with frequencies

$$\tilde{\omega}_\pm = \frac{1}{2}(-\omega_4 - \xi \pm \sqrt{(\omega_4+\xi)^2 + 4\Omega^2}) \tag{41}$$

and the first factor is a sum of a time-independent and an oscillating projection operators, the frequency of the latter being $\omega_4 + \xi$. Thus, $U_c(t)$ is a sum of four oscillating terms with frequencies $\pm\tilde{\omega}_+$, $\pm\tilde{\omega}_-$ and is T_c-periodic provided both $\tilde{\omega}_+T_c$ and $\tilde{\omega}_-T_c$ are integer multiples of 2π.

Under this prescription, $[U_c^\dagger(t)\otimes\mathbf{1}_B]H_{SB}[U_c(t)\otimes\mathbf{1}_B]$ is a sum of terms proportional to $e^{\pm i\tilde{\omega}_+t}, e^{\pm i\tilde{\omega}_-t}$, $e^{\pm 2i\omega_3't}e^{\pm i\tilde{\omega}_+t}$, $e^{\pm 2i\omega_3't}e^{\pm i\tilde{\omega}_-t}$, and its average vanishes in the $T_c \to 0$ limit:

$$\lim_{T_c\to 0}\frac{1}{T_c}\int_0^{T_c} dt(U_c^\dagger(t) \otimes \mathbf{1}_B)H_{SB}(U_c(t) \otimes \mathbf{1}_B) = 0. \tag{42}$$

Therefore, the general argument of section 2 shows that the coupling between the system and the reservoir is suppressed in the limit $T_c \to 0$ (i.e., $\tilde{\omega}_\pm \to \infty$) while keeping $T = NT_c$ constant. Moreover, the system obeys the Hamiltonian

$$\bar{H}_s = \frac{1}{T_c}\int_0^{T_c} dt U_c^\dagger(t)\{\omega_4|4\rangle\langle 4| + \lambda^2 H_S^R\}U_c(t)$$
$$= \omega_4\sum_{s=\pm}\tilde{\omega}_s^2\frac{(\Omega|3\rangle + \tilde{\omega}_s|4\rangle)(\Omega\langle 3| + \tilde{\omega}_s\langle 4|)}{(\Omega^2+\tilde{\omega}_s^2)^2} + \lambda^2 H_S^R. \tag{43}$$

Therefore, the target system spanned by $|1\rangle$ and $|2\rangle$ is free from decoherence and performs ideal Rabi oscillations.

It is interesting to see the relation between the dynamical decoupling and a dynamical quantum Zeno effect due to a "continuous" measurement [20]. For the particular choice (37), it is possible to eliminate the explicit time dependence of the control Hamiltonian H_c, by going to another rotating frame with the aid of the unitary operator

$$U_R^b(t) = \exp\{i(\omega_4+\xi)|4\rangle\langle 4|t\} \otimes \mathbf{1}_B. \tag{44}$$

Then, the transformed density matrix $\bar{\rho} = U_R^b(t)\rho U_R^{b\dagger}(t)$ obeys

$$\frac{\partial\bar{\rho}}{\partial t} = \{\mathcal{L}_B + \Delta\mathcal{L}_S' + \mathcal{L}_c' + \lambda\mathcal{L}_{SB} + \lambda^2\mathcal{L}_S\}\bar{\rho}, \tag{45}$$

where the transformed control Liouvillian is

$$(\Delta\mathcal{L}_S' + \mathcal{L}_c')\rho = [\{-\xi|4\rangle\langle 4| + \Omega[|3\rangle\langle 4| + (h.c.)]\} \otimes \mathbf{1}_B, \rho]. \tag{46}$$

In this picture, state $|4\rangle$ of energy $-\xi$ is coupled by a constant coupling Ω to state $|3\rangle$. The short-period limit $T_c \to 0$ corresponds to the strong coupling limit Ω, $\xi \to \infty$, because $\tilde{\omega}_\pm T_c$ must be integer multiples of 2π. But this is just the case of a dynamical quantum Zeno effect due to a continuous measure-

ment [20], where $H_{\text{meas}} = -\xi|4\rangle\langle 4| + \Omega\{|3\rangle\langle 4| + (h.c.)\}$ plays the role of a measurement Hamiltonian. One can show that, in the limit of strong coupling, a dynamical superselection rule arises, the Hilbert space is split into Zeno subspaces, and the system Hamiltonian is given again by (12), where the projections P_ns, defining the Zeno subspaces, are the eigenprojections of H_{meas} [20]. This is a consequence of an interesting relation between strong-coupling regime and adiabatic evolution [22].

The eigenprojections of H_{meas} are given by $P_\pm = |\pm\rangle\langle\pm|$, where

$$|\pm\rangle = \frac{\Omega|3\rangle + \omega_\pm|4\rangle}{\sqrt{\Omega^2 + \omega_\pm^2}}, \tag{47}$$

with eigenvalues

$$\omega_\pm = \tfrac{1}{2}(-\xi \pm \sqrt{\xi^2 + 4\Omega^2}). \tag{48}$$

Therefore, from (12) one gets

$$\begin{aligned}\bar{H}_s &= \sum_{s=\pm} P_s(-\xi|4\rangle\langle 4| + \lambda^2 H_S^R) P_s \\ &= -\xi \sum_{s=\pm} \omega_s^2 \frac{(\Omega|3\rangle + \omega_s|4\rangle)(\Omega\langle 3| + \omega_s\langle 4|)}{(\Omega^2 + \omega_s^2)^2} + \lambda^2 H_S^R,\end{aligned} \tag{49}$$

which is nothing but the Hamiltonian (43) under the transformation (44). We see that, in this particular case, dynamical decoupling is completely equivalent to the dynamical Zeno effect.

4.2. NONIDEAL DYNAMIC DECOUPLING

Here we consider the case of nonvanishing T_c and solve the evolution equation (39). As pointed out in [11, 14], the ideal dynamical decoupling is achieved when the control frequency $2\pi/T_c$ is higher than the threshold frequency ω_c in the system–reservoir interaction H_{SB} and, thus, we consider the case where $2\pi/T_c = O(\lambda^0)$. Then, the slow process which is relevant to the quantum state manipulation is well described by the van Hove limit approximation [24–26].

We consider the evolution in the rotated frame (45). Note that because the transformation U_R^b in (44) does not affect the evolution of the states $|j\rangle$ ($j = 1, 2$) and the field variable, one has $\langle i|\mathrm{tr}_B\rho|j\rangle = \langle i|\mathrm{tr}_B\bar{\rho}|j\rangle$ ($i, j = 1, 2$). By the standard procedure of the van Hove limit approximation [24, 25], in the limit $\lambda \to 0$, while keeping $\tau = \lambda^2 t$ constant, one obtains

$$\frac{\partial \sigma}{\partial \tau} = -i\Lambda_B \sigma, \tag{50}$$

where $\sigma(\tau) \equiv \mathrm{tr}_B\bar{\rho}$ and

$$\begin{aligned}-i\Lambda_B\sigma = &-i\left[\sum_{s=\pm} \delta_s|s\rangle\langle s| + \Delta[|1\rangle\langle 2| + (h.c.)], \sigma\right] \\ &+ \sum_{s=\pm} (\gamma_e^s|1\rangle\langle s|\sigma|s\rangle\langle 1| + \gamma_d^s|s\rangle\langle 1|\sigma|1\rangle\langle s|) \\ &- \left\{\frac{\gamma_d^B}{2}|1\rangle\langle 1| + \sum_{s=\pm}\frac{\gamma_e^s}{2}|s\rangle\langle s|, \sigma\right\}.\end{aligned} \tag{51}$$

The states $|\pm\rangle$ are the normalized linear combinations of the states $|3\rangle$ and $|4\rangle$ given by (47) and the decay rates γ_e^s and γ_d^s ($s = \pm$) and γ_d^B are given by

$$\begin{aligned}\gamma_d^B &= \gamma_d^+ + \gamma_d^-, \\ \gamma_{d/e}^\pm &= 2\pi \frac{|\omega_\mp|}{\omega_+ - \omega_-}\kappa_{d/e}(\omega_3' + \omega_\pm),\end{aligned} \tag{52}$$

where $\omega_\pm$ are the frequencies (48) and $\kappa_{d/e}(\omega)$ are the thermal form factors (32), extended to the whole real axis due to the counterrotating terms. (Incidentally, note the exchange symmetry $\kappa_e(\omega) = \kappa_d(-\omega)$ of the extended form factors.)

The prefactors in the second equation in (52) are nothing but the squares of the matrix elements between the undressed state $|3\rangle$ and the dressed states $|\pm\rangle$ (47):

$$\frac{|\omega_\mp|}{\omega_+ - \omega_-} = |\langle 3|\pm\rangle|^2. \tag{53}$$

The explicit expressions of the Lamb shifts δ_s ($s = \pm$) of the excited states are omitted since the relevant sector of the evolution equation does not depend on them. Note that the parameter δ is chosen so that the operator Λ_B does not contain a commutator with $|1\rangle\langle 1|$.

In terms of the matrix elements $\sigma_{ij} \equiv \langle i|\sigma|j\rangle$, one has

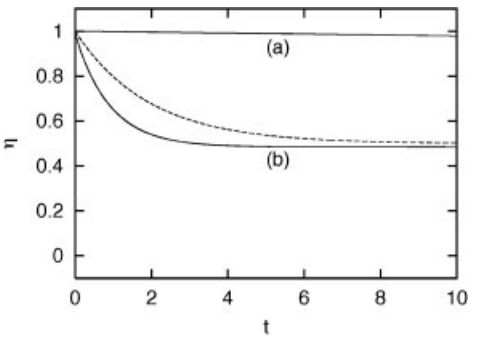

FIGURE 4. Evolution of the purity η of the system state. The time unit in the horizontal axis is the decoherence time γ_d^{-1} for the uncontrolled case. (a) Control frequency $|\omega_-| = 150 \times \omega_3'$; (b) control frequency $|\omega_-| = 0.5 \times \omega_3'$. For comparison, the behavior of η without control is also displayed (broken curve).

$$\frac{\partial \sigma_{11}}{\partial \tau} = -i\Delta\{\sigma_{21} - \sigma_{12}\} - \gamma_d^B \sigma_{11} + \sum_{s=\pm} \gamma_e^s \sigma_{ss} \quad (54)$$

$$\frac{\partial \sigma_{12}}{\partial \tau} = -i\Delta\{\sigma_{22} - \sigma_{11}\} - \frac{\gamma_d^B}{2}\sigma_{12} \quad (55)$$

$$\frac{\partial \sigma_{22}}{\partial \tau} = i\Delta\{\sigma_{21} - \sigma_{12}\} \quad (56)$$

$$\frac{\partial \sigma_{ss}}{\partial \tau} = \gamma_d^s \sigma_{11} - \gamma_e^s \sigma_{ss} \cdot (s = \pm). \quad (57)$$

The evolution of the purity $\eta = \sigma_{11}^2 + \sigma_{22}^2 + 2|\sigma_{12}|^2$ of the target states is shown in Figure 4 for different values of control parameters, where the parameters in the control Hamiltonian are set to $\xi = 24\Omega/5$ (which gives $\omega_+ = \Omega/5$ and $\omega_- = -5\Omega$), the frequency cutoff to $\omega_c = 10\omega_3'$, and the other parameters are chosen, so that one has $\Delta = 100\gamma_d$ and $\gamma_e = 1000\gamma_d$ for the uncontrolled case. As in the previous section, the initial state is $\sigma(0) = |1\rangle\langle 1|$. Figure 4 shows that the dynamical decoupling control may accelerate decoherence if the parameters are not appropriately tuned.

Figure 5 shows the control frequency dependence of the decoherence rate γ_d^B. As can be seen in Figure 4, decoherence is first enhanced, for small values of $|\omega_-| = 5\Omega$, and then suppressed for much larger values of $|\omega_-|$. Since the decoherence rate γ_d^+ due to $|+\rangle$ is a monotonically decreasing function of $|\omega_-|$, this can be understood as follows: In the rotating frame where the $|3\rangle - |4\rangle$ oscillation is eliminated, when $\Omega = 0$, state $|3\rangle$ is separated from the decay product state $|1\rangle$ by an energy ω_3'. When Ω is turned on, state $|3\rangle$ splits into two dressed states $|\pm\rangle$, which are separated from $|1\rangle$ by the energies $\omega_3' + \omega_+ \equiv \omega_3' + |\omega_-|/25$ and $\omega_3' - |\omega_-|$, respectively. The latter state is closer to state $|1\rangle$ than in the uncontrolled case and leads to a shorter decoherence time provided $\omega_3' - |\omega_-| > 0$. This is the deterioration observed in Figure 4, case (b). In contrast, if $|\omega_-|$ exceeds a threshold energy $\omega_{th} \equiv \omega_3'$, the energy of state $|-\rangle$ becomes lower than that of state $|1\rangle$. In such a case, the counterrotating term (which are now "rotating") does contribute to the decoherence rate. Note that now, being $\omega_3' - |\omega_-| < 0$, γ_e^- is smaller than γ_d^-, as it should. Even after $|\omega_-|$ has exceeded the threshold, ω_{th}, γ_d^- still increases with $|\omega_-|$, as the state $|1\rangle$ is now unstable. Finally, when energies of the two dressed states are sufficiently far apart from that of level $|1\rangle$, the decay rates (and therefore decoherence) are suppressed because of the high-energy cutoff of the form factor (17). Such values of $|\omega_-| \sim 80\omega_3'$ are considerably higher than the threshold $\omega_{th} = \omega_3'$ (Fig. 5) and involve extremely short timescales [28].

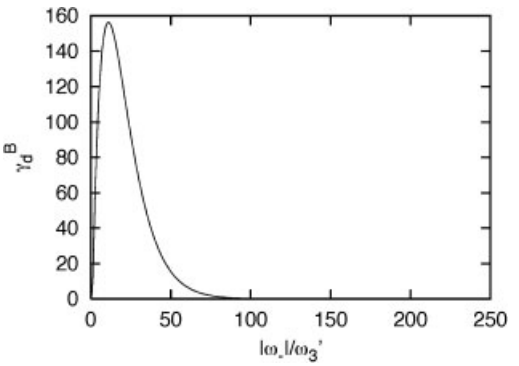

FIGURE 5. Decoherence rate γ_d^B vs control frequency $|\omega_-|/\omega_3'$.

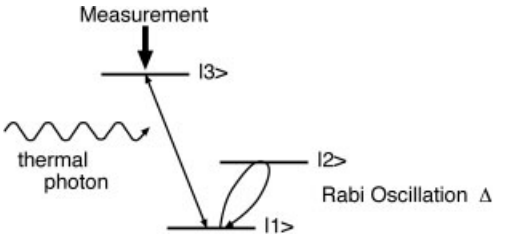

FIGURE 6. Schematic representation of the system under the quantum Zeno control.

5. Quantum Zeno Control of Thermal Decoherence

For the same reason as in the dynamical decoupling, we disturb the evolution of $|3\rangle$ by repeated measurements (Fig. 6). The nonselective measurement of $|3\rangle$ causes the following change of the density matrix:

$$\rho \rightarrow \hat{P}\rho \equiv \pi_3\rho\pi_3 + (\mathbf{1} - \pi_3)\rho(\mathbf{1} - \pi_3) \quad (58)$$

where π_3 is a projection operator acting on the whole Hilbert space $\pi_3 \equiv |3\rangle\langle 3| \otimes \mathbf{1}_B$ and $\mathbf{1} = \mathbf{1}_S \otimes \mathbf{1}_B$. Then, the density matrix under the Zeno control is given by

$$\rho(NT_c) = \prod_{m=1}^{N} \{\hat{P}\mathcal{T}e^{-i\int_{(m-1)T_c}^{mT_c}\mathcal{L}_{\mathrm{tot}}(t)dt}\hat{P}\}\rho(0), \quad (59)$$

where T_c stands for the time interval between successive measurements.

5.1. IDEAL ZENO CONTROL

First, we consider the case where $T_c \rightarrow 0$, while keeping $T = NT_c$ constant. Then, because $\hat{P}H_{SB} = \pi_3 H_{SB}\pi_3 + (\mathbf{1} - \pi_3)H_{SB}(\mathbf{1} - \pi_3) = 0$, and as discussed in section 2, the state at time T is given by

$$\rho(T) = \hat{P}(e^{-iH_S'T} \otimes e^{-iH_BT}\rho(0)e^{iH_S'T} \otimes e^{iH_BT}), \quad (60)$$

where the controlled system Hamiltonian $\bar{H}_S'$ is given by

$$\begin{aligned}\bar{H}_S' &= \lambda^2\{P_3H_S^RP_3 + (\mathbf{1}_S - P_3)H_S^R(\mathbf{1}_S - P_3)\} \\ &= \lambda^2\{-\delta|1\rangle\langle 1| + [\Delta|1\rangle\langle 2| + (h.c.)]\},\end{aligned} \quad (61)$$

with $P_3 = |3\rangle\langle 3|$. Hence, as a result of infinitely frequent measurements of state $|3\rangle$, the system–reservoir coupling is eliminated and, thus, decoherence is suppressed.

5.2. NONIDEAL ZENO CONTROL

As in the dynamical decoupling, we consider the case in which $T_c \sim 1/\omega_3' \sim \lambda^0$, so that the time evolution is well described by the van Hove limit where $\lambda \rightarrow 0$, while keeping $\tau = \lambda^2 NT_c$ and T_c constant. In this case, we are looking at the subtle effects on the decay rate that arise from the presence of a short-time quadratic (Zeno) region. Therefore, it is important to note that the standard method [24, 25] is not applicable to the present situation, and the limit is evaluated as follows:

1. Second-order perturbation, up to λ^2, and $\hat{P}H_{SB} = 0$ lead to

$$\begin{aligned}\hat{P}\mathcal{T}e^{-i\int_{mT_c}^{(m+1)T_c}\mathcal{L}_{\mathrm{tot}}(t)dt}\hat{P} \simeq \hat{P}e^{-i\mathcal{L}_BT_c}\Bigg\{\mathbf{1} - i\lambda^2\mathcal{L}_ST_c - \lambda^2 \\ \times\int_{mT_c}^{(m+1)T_c}dt\int_{mT_c}^{t}ds e^{i\mathcal{L}_Bt}\mathcal{L}_{SB}(t)e^{-i\mathcal{L}_B(t-s)}\mathcal{L}_{SB}(s)e^{-i\mathcal{L}_Bs}\hat{P}\Bigg\}\end{aligned} \quad (62)$$

2. In terms of the operator $\mathcal{K}_m$, defined as a solution of the operator equation

$$\begin{aligned}\hat{P}\int_{mT_c}^{(m+1)T_c}dt\int_{mT_c}^{t}ds e^{i\mathcal{L}_Bt}\mathcal{L}_{SB}(t) \\ \times e^{-i\mathcal{L}_B(t-s)}\mathcal{L}_{SB}(s)e^{-i\mathcal{L}_Bs}\hat{P} \\ = \hat{P}\int_{mT_c}^{(m+1)T_c}dt e^{i\mathcal{L}_Bt}\mathcal{K}_m e^{-i\mathcal{L}_Bt},\end{aligned} \quad (63)$$

one has

$$\begin{aligned}&\hat{P}\mathcal{T}e^{-i\int_{mT_c}^{(m+1)T_c}\mathcal{L}_{\mathrm{tot}}(t)dt}\hat{P} \\ &\simeq \hat{P}\mathcal{T}e^{-i\int_{mT_c}^{(m+1)T_c}[\mathcal{L}_B+\lambda^2\mathcal{L}_S-i\lambda^2\mathcal{K}(t)]dt} + O(\lambda^3),\end{aligned} \quad (64)$$

where

$$\mathcal{K}(t) = \mathcal{K}_m \quad \text{for} \quad mT_c \le t < (m+1)T_c.$$

3. With the aid of (64) and $\hat{\rho}\sigma \equiv P_3\sigma P_3 + (\mathbf{1}_S - P_3)\sigma(\mathbf{1}_S - P_3)$, the final reduced state $\sigma(\tau)$ is given by

$$\begin{aligned}&\sigma(\tau) = \\ &\lim_{\substack{\lambda\rightarrow 0 \\ \tau=\lambda^2NT_c:\mathrm{finite}}} \mathrm{tr}_B\Bigg\{\prod_{m=1}^{N}[\hat{P}\mathcal{T}e^{-i\int_{(m-1)T_c}^{mT_c}\mathcal{L}_{\mathrm{tot}}(t)dt}\hat{P}]\sigma(0) \otimes \rho_B\Bigg\} \\ &= \hat{\rho}\lim_{\substack{\lambda\rightarrow 0 \\ \tau=\lambda^2NT_c:\mathrm{finite}}} \mathrm{tr}_B\rho^*(NT_c).\end{aligned} \quad (65)$$

where

$$\rho^*(NT_c) = \hat{P}\mathcal{T}e^{-i\int_0^{NT_c}(\mathcal{L}_B+\lambda^2\mathcal{L}_S-i\lambda^2\mathcal{K}(t))dt}\sigma(0) \otimes \rho_B.$$

4. As $\rho^*(t)$ is a solution of

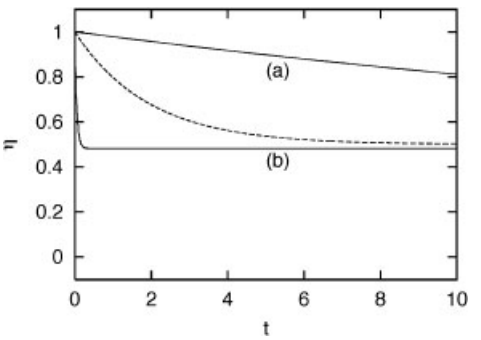

FIGURE 7. Evolution of the purity η of the target states. The time unit on the horizontal axis is the decoherence time γ_d^{-1} for the uncontrolled case. (a) Control frequency $2\pi/T_c = 5 \times 10^6 \times \omega_3'$; (b) control frequency $2\pi/T_c = 0.5 \times \omega_3'$. For comparison, the behavior of η without control is also displayed by a broken curve.

$$\frac{\partial \rho^*(t)}{\partial t} = -i[\mathcal{L}_B + \lambda^2 \mathcal{L}_S - i\lambda^2 \mathcal{K}(t)]\rho^*(t),$$

$$\rho^*(0) = \sigma(0) \otimes \rho_B, \tag{66}$$

the standard van Hove limit arguments [24, 25] show that $\sigma(\tau) = \hat{p}\sigma^*(\tau)$ and σ^* satisfies

$$\frac{\partial \sigma^*(\tau)}{\partial \tau} = -i\,\mathrm{tr}_B\{(\mathcal{L}_S - i\mathcal{K})\sigma^*(\tau) \otimes \rho_B\}$$

$$\sigma^*(0) = \sigma(0), \tag{67}$$

where the time dependence of $\mathcal{K}$ is lost as a result of the partial trace.

As in the previous sections, the parameter δ is chosen so that the $|1\rangle\langle 1|$-term does not appear in the evolution operator of σ^*. In terms of the matrix elements $\sigma_{ij}^* \equiv \langle i|\sigma^*|j\rangle$, (67) reads

$$\frac{\partial \sigma_{11}^*}{\partial \tau} = -i\Delta\{\sigma_{21}^* - \sigma_{12}^*\} - \gamma_d^Z \sigma_{11}^* + \gamma_e^Z \sigma_{33}^* \tag{68}$$

$$\frac{\partial \sigma_{12}^*}{\partial \tau} = -i\Delta\{\sigma_{22}^* - \sigma_{11}^*\} - \frac{\gamma_d^Z}{2}\sigma_{12}^* \tag{69}$$

$$\frac{\partial \sigma_{22}^*}{\partial \tau} = i\Delta\{\sigma_{21}^* - \sigma_{12}^*\} \tag{70}$$

$$\frac{\partial \sigma_{33}^*}{\partial \tau} = \gamma_d^Z \sigma_{11}^* - \gamma_e^Z \sigma_{33}^* \tag{71}$$

where the decoherence rate γ_d^Z and the inverse lifetime γ_e^Z of $|3\rangle$ are given by

$$\gamma_d^Z = T_c \int_{-\infty}^{\infty} d\omega \kappa_d(\omega) \mathrm{sinc}^2\left(\frac{\omega - \omega_3'}{2} T_c\right) \tag{72}$$

$$\gamma_e^Z = T_c \int_{-\infty}^{\infty} d\omega \kappa_e(\omega) \mathrm{sinc}^2\left(\frac{\omega - \omega_3'}{2} T_c\right), \tag{73}$$

where $\kappa_{d/e}(\omega)$ are again the (extended) thermal form factors (32) and $\mathrm{sinc}(x) = (\sin x)/x$. The decay rate γ_d^Z in (72) should be compared with γ_d^B in (52). They express the (inverse) quantum Zeno effect, given by pulsed or continuous measurement, respectively [19].

Because the projection operator $\hat{p}$ does not affect the $|1\rangle - |2\rangle$ sector, one has $\sigma_{ij}^*(\tau) = \langle i|\sigma(\tau)|j\rangle$ for a class of initial states where only the matrix elements $\langle i|\sigma(0)|j\rangle$ $(i, j = 1, 2)$ are nonvanishing. Hence, $\eta = {\sigma_{11}^*}^2 + {\sigma_{22}^*}^2 + 2|\sigma_{12}^*|^2$ measures the purity of the target states. Its evolution is shown in Figure 7 for different values of $2\pi/T_c$, where $\omega_c = 10\omega_3'$ and the other parameters are chosen so that one has $\Delta = 100\gamma_d$ and $\gamma_e = 1000\gamma_d$ for the uncontrolled case. As in the previous sections, the initial state is $\sigma(0) = |1\rangle\langle 1|$. Figure 7 shows that the Zeno control may accelerate decoherence if the parameters are not appropriately chosen. This can be seen more clearly in the control-frequency dependence of the decoherence rate γ_d^Z, which is shown in Figure 8. When the control frequency $2\pi/T_c$ belongs to a certain range, decoherence is enhanced.

The enhancement of decoherence is qualitatively similar to the case of dynamical decoupling. However, the high-frequency behavior of the decoher-

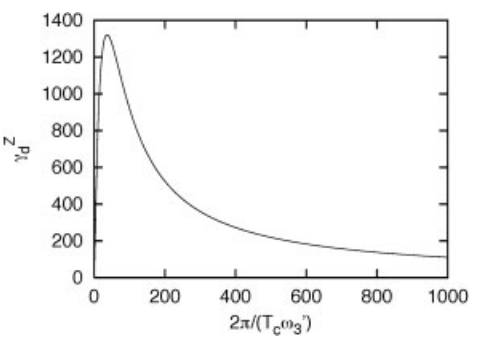

FIGURE 8. Decoherence rate γ_d^Z vs control frequency $2\pi/(T_c\omega_3')$.

ence rate and its peak values are quite different. The high-frequency decoherence rates γ_d^B and γ_d^Z, respectively, for the dynamical decoupling and Zeno control, are approximated by

$$\gamma_d^B \simeq \frac{\omega_+ \gamma_e \omega_c}{\omega_3'(\omega_+ - \omega_-)} \frac{|\omega_-|}{\omega_c} e^{-(|\omega_-|/\omega_c)}$$

$$\gamma_d^Z \simeq \frac{\gamma_e}{\left(\frac{2\pi}{\omega_3' T_c}\right)} \left(\frac{\omega_c}{\omega_3'}\right)^2. \quad (74)$$

Therefore, γ_d^B decays exponentially for large $|\omega_-|$ because of the exponential cutoff of the form factor and may take a maximum of order $\omega_+ \gamma_e \omega_c / \{e(\omega_+ - \omega_-)\omega_3'\} \sim 140$. In contrast, γ_d^Z decays polynomially for large $2\pi/T_c$ and γ_d^Z could be much larger than γ_d^B because $\gamma_e \omega_c^2 / \omega_3'^2 \sim 10^5$ is very large.

6. Conclusions

We have studied the dynamical decoupling and Zeno controls for a model of trapped ions, where decoherence appears in the dynamics of the hyperfine states due to emission and absorption of thermal photons associated with the transition between the lower hyperfine and an excited state. By very rapidly driving or very frequently measuring the excited state, decoherence is shown to be suppressed. However, if the frequency of the controls is not high enough, the controls may accelerate the decoherence process and may deteriorate the performance of the quantum state manipulation.

The acceleration of decoherence is analogous to the inverse Zeno effect, namely the acceleration of the decay of an unstable state due to frequent measurements [27]. In the original discussion of the Zeno effect [16–19], very frequently repeated measurements of an unstable state is shown to slow down its decay. But, if the duration between two successive measurements is not short enough, the frequent measurements may accelerate the decay. This is the inverse Zeno effect. Obviously, this situation precisely corresponds to the increase of decoherence observed in this article. Moreover, since a very intense field is used for the dynamical decoupling control, the decrease of the decoherence time is also a consequence of the decrease of the lifetime of the unstable states due to the intense field [28].

There is room for improvement and further analysis: a number of neglected effects can be considered, such as the role of counterrotating terms and Fano states, the influence of the other atomic states, the primary importance of the relevant timescales and so on. These aspects will be discussed elsewhere.

ACKNOWLEDGMENTS

It is a privilege for one of the authors (S. T.) to dedicate this article to Professor Ilya Prigogine on the occasion of his 85th birthday, particularly because the first work of S. T. with Professor Prigogine was on the quantum Zeno effect [18]. S. T. worked with Professor Prigogine and his group from 1989 to 1993 as a postdoc and is indebted to him for strong support and encouragement as well as all about science, which S. T. learnt in Brussels. S. T. also thanks Professors I. Antoniou, R. Lefever, and A. Goldbeter and La Fondations des Treilles for their invitation to the Workshop on "Complexity: microscopic and macroscopic aspects" and their warm hospitality. The authors are grateful to Professors I. Antoniou, B. Misra, A. Takeuchi, I. Ohba, H. Nakazato, L. Accardi, T. Hida, M. Ohya, K. Yuasa, and N. Watanabe for fruitful discussions and comments. This work is supported by a Grant-in-Aid for Scientific Research (C) from JSPS and by a Grant-in-Aid for Scientific Research of Priority Areas, Control of Molecules in Intense Laser Fields, from the Ministry of Education, Culture, Sports, Science, and Technology of Japan.

References

1. Galindo, A.; Martin-Delgado, M. A. Rev Mod Phys 2002, 74, 347; Bouwmeester, D.; Ekert, A.; Zeilinger, A., Eds. The Physics of Quantum Information; Springer: Berlin, 2000; Nielsen, M. A.; Chuang, I. L. Quantum Computation and Quantum Information; Cambridge University Press: Cambridge, UK, 2000.
2. Shor, P. W. Proceedings of the Thirty-five Annual Symposium on the Foundations of Computer Science; IEEE Computer Society Press: Los Alamos, CA, 1996; Ekert, A.; Jozsa, R. Rev Mod Phys 1996, 68, 733.
3. Grover, L. K. Proceedings of the Twenty-eighth Annual ACM Symposium on the Theory of Computing, Philadelphia; Association for Computing Machinery: New York, 1996, p. 212; Phys Rev Lett 1997, 79, 325.
4. Monroe, C.; Meekhof, D. M.; King, B. E.; Itano, W. M.; Wineland, D. J. Phys Rev Lett 1995, 75, 4714.
5. Hughes, R. J.; James, D. F. V.; Gomez, J. J.; Gulley, M. S.; Holzscheiter, M. H.; Kwiat, P. G.; Lamoreaux, S. K.; Peterson,

C. G.; Sandberg, V. D.; Schauer, M. N.; Simmons, C. M.; Thorburn, C. E.; Tupa, D.; Wang, P. Z.; White, A. G. Fortschr Phys 1998, 46, 32.

6. e.g., see Cory, D. G.; Laflamme, R.; Knill, E.; Viola, L.; Havel, T. F.; Boulant, N.; Boutis, G.; Fortunato, E.; Lloyd, S.; Martinez, R.; Negrevergne, C.; Pravia, M.; Sharf, Y.; Teklemariam, G.; Weinstein, Y. S.; Zurek, W. H. Fortschr Phys 2000, 48, 875.
7. Lieven, M.; Vandersypen, K.; Steffen, M.; Breyta, G.; Yannoni, C. S.; Sherwood, M. H.; Chuang, I. L. Nature 2001, 414, 883.
8. Unruh, W. G. Phys Rev A 1995, 51, 992; see also Chuang, I. L.; Laflamme, R.; Shor, P. W.; Zurek, W. H. Science 1995, 270, 1633; Zurek, W. H.; Paz, J. P. Nuovo Cimento Soc Ital 1995, 110B, 611.
9. Shor, P. W. Phys Rev A 1995, 52, 2493; Calderbank, A. R.; Shor, P. W. Phys Rev A 1996, 54, 1098; Steane, A. Proc R Lond A 1996, 452, 2551; Steane, A. Phys Rev Lett 1996, 77, 793.
10. Duan, L. M.; Guo, G. C. Phys Rev Lett 1997, 79, 1953; Zanardi, P.; Rasetti, M. Phys Rev Lett 1997, 79, 3306; Lidar, D. A.; Chuang, I. L.; Whaley, K. B. Phys Rev Lett 1998, 81, 2594; Knill, E.; Laflamme, R.; Viola, L. Phys Rev Lett 2000, 84, 2525.
11. Viola, L.; Lloyd, S. Phys Rev A 1998, 58, 2733.
12. Viola, L.; Knill, E.; Lloyd, S. Phys Rev Lett 1999, 82, 2417.
13. Viola, L.; Lloyd, S.; Knill, E. Phys Rev Lett 1999, 83, 4888; Viola, L.; Knill, E.; Lloyd, S. Phys Rev Lett 2000, 85, 3520; Zanardi, P. Phys Lett A 1999, 258, 77.
14. Vitali, D.; Tombesi, P. Phys Rev A 1999, 59, 4178; Phys Rev A 2001, 65, 012305.
15. Byrd, M. S.; Lidar, D. A. Quantum Information Processing 2002, 1, 19; Empirical Determination of Bang-Bang Operations, quant-ph/0205156.
16. von Neumann, J. Mathematical Foundation of Quantum Mechanics; Princeton University Press: Princeton, NJ, 1955; Beskow, A.; Nilsson, J. Ark Fys 1967, 34, 561; Khalfin, L. A. JETP Lett 1968, 8, 65; Misra, B.; Sudarshan, E. C. G. J Math Phys 1977, 18, 756; Peres, A. Am J Phys 1980, 48, 931; Kraus, K. Found Phys 1981, 11, 547; Sudbery, A. Ann Phys 1984, 157, 512; Cook, R. J. Phys Scr T 1988, 21, 49.
17. Itano, W. M.; Heinzen, D. J.; Bolinger, J. J.; Wineland, D. J. Phys Rev A 1990, 41, 2295.
18. Petrosky, T.; Tasaki, S.; Prigogine, I. Phys Lett A 1990, 151, 109; Physica A 1991, 170, 306.
19. Home, D.; Whitaker, M. A. B. Ann Phys 1997, 258, 237; Facchi, P.; Pascazio, S. Progress in Optics; Vol. 42. Wolf, E., Ed.; Elsevier: Amsterdam, 2001, p. 147.
20. Facchi, P.; Pascazio, S. Phys Rev Lett 2002, 89, 080401; Quantum Zeno Subspaces and Dynamical Superselection Rules, quant-phys/0207030, 2002; Facchi, P.; Gorini, V.; Marmo, G.; Pascazio, S.; Sudarshan, E. C. G. Phys Lett A 2000, 275, 12.
21. Schwinger, J. Proc Natl Acad Sci USA 1959, 45, 1552; Quantum Kinetics and Dynamics; W. A. Benjamin: New York, 1970.
22. Frasca, M. Phys Rev A 1998, 58, 3439.
23. Wilcox, R. M. J Math Phys 1967, 8, 962.
24. van Hove, L. Physica 1957, 23, 441; Nakajima, S. Prog Theor Phys 1958, 20, 948; Prigogine, I.; Résibois, P. Physica 1961, 27, 629; Zwanzig, R. J Chem Phys 1960, 33, 1338; Davies, E. B. Quantum Theory of Open Systems; Academic Press: New York, 1976.
25. Spohn, H.; Lebowitz, J. L. Adv Chem Phys 1979, 38, 109.
26. Kimura, G.; Yuasa, K.; Imafuku, K. Phys Rev A 2001, 63, 022103; Phys Rev Lett 2002, 89, 140403.
27. Lane, A. M. Phys Lett A 1983, 99, 359; Schieve, W. C.; Horwitz, L. P.; Levitan, J. Phys Lett A 1989, 136, 264; Kofman, A. G.; Kurizki, G. Nature 2000, 405, 546; Elattari, B.; Gurvitz, S. A. Phys Rev A 2000, 62, 032102; Facchi, P.; Nakazato, H.; Pascazio, S. Phys Rev Lett 2001, 86, 2699.
28. Facchi, P.; Pascazio, S. Phys Rev A 2000, 62, 023804.